GRAVITATIONAL REDSHIFT OF EMISSION LINES IN THE AGN SPECTRA

N. Bon, E. Bon & L. Č. Popović

10th SCSLSA, Srebrno Jezero, 15-19. Jun 2015.

Gravitationally redshifted emission line

Popović et al. 1995

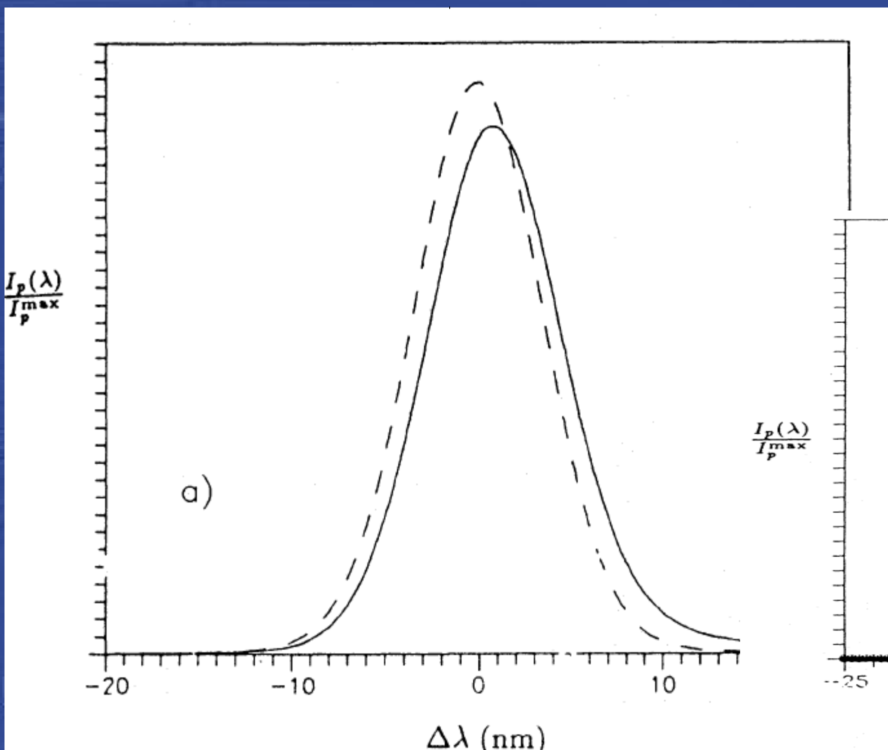

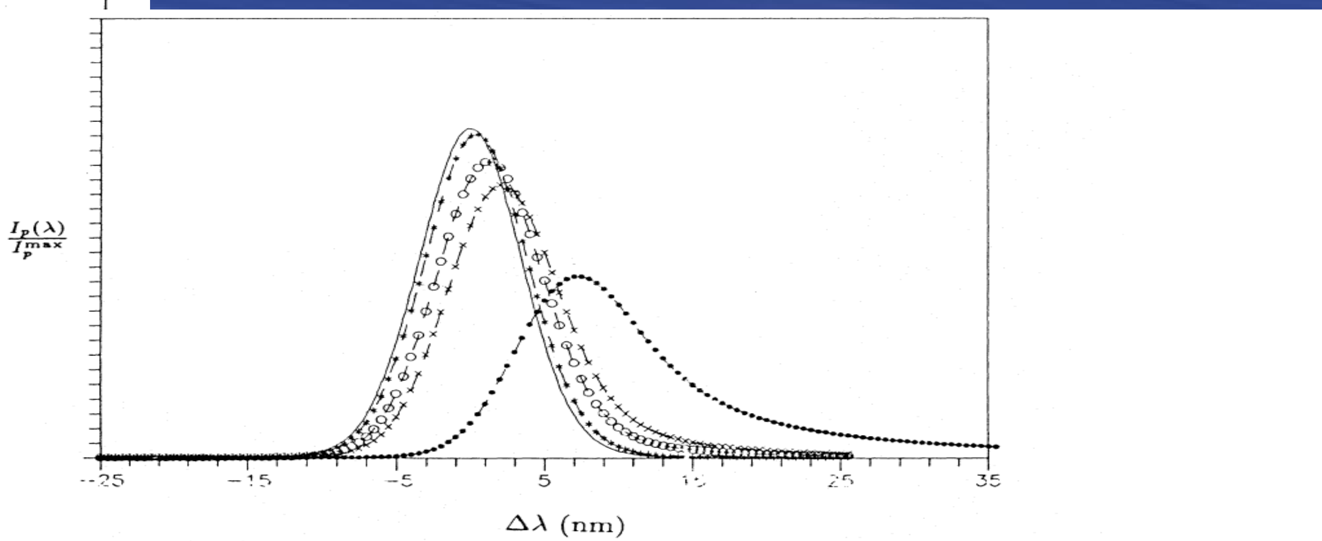

Fig. 3. The shape of spectral line for different transition wavelengths λ_0 = 100 nm (∗ − ∗−), λ_0 = 500 nm (○ − ○−), λ_0 = 1000 nm (× − ×−) and λ_0 = 5000 nm (• − •−) in comparison with the nondeformed profile (full line)

Gravitationally deformed Hβ line profile (full line) in comparison with the non-deformed Voight profile (dashed line) for the typical broad emission line

Variability of AGN emission lines

NGC 5548

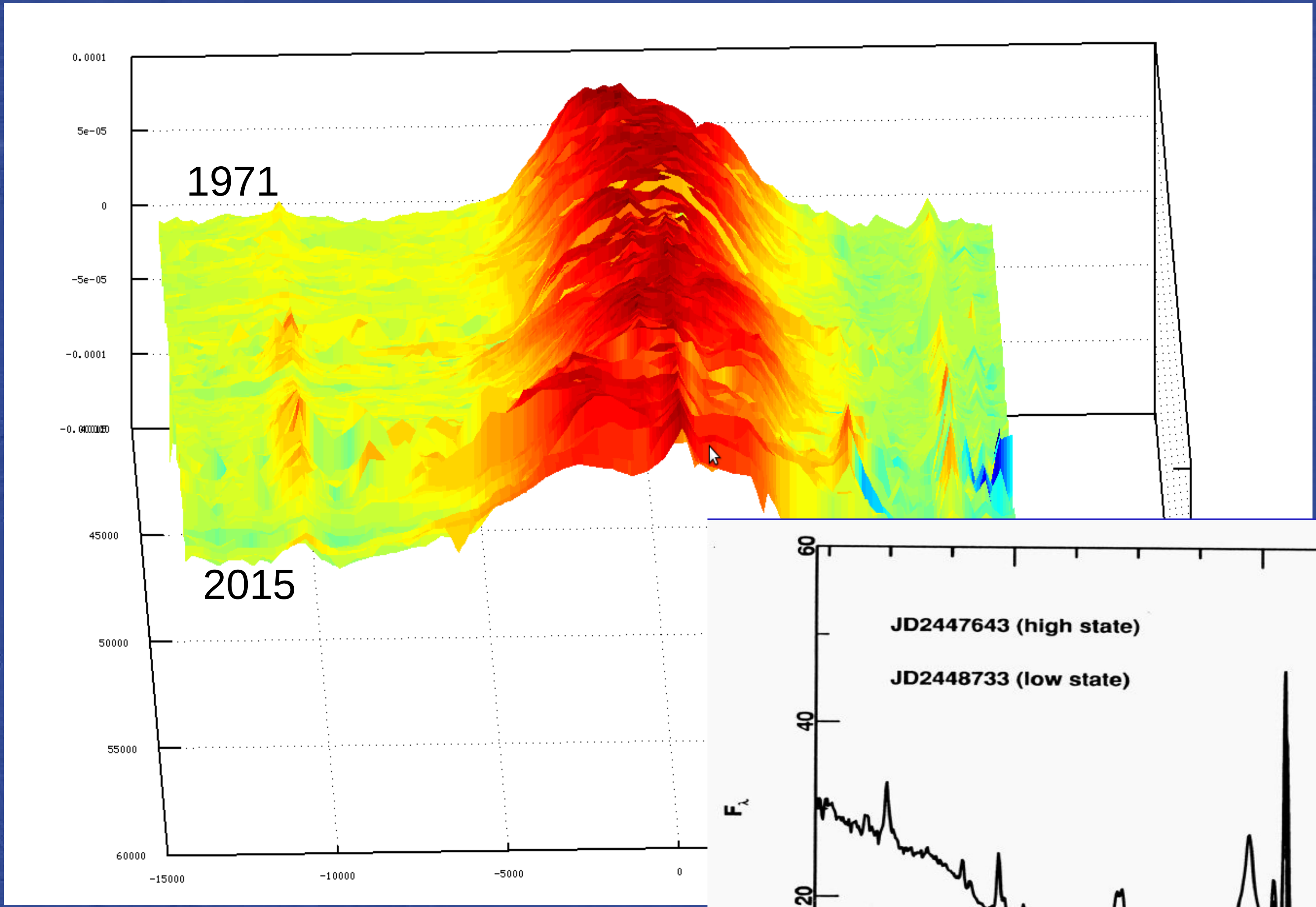

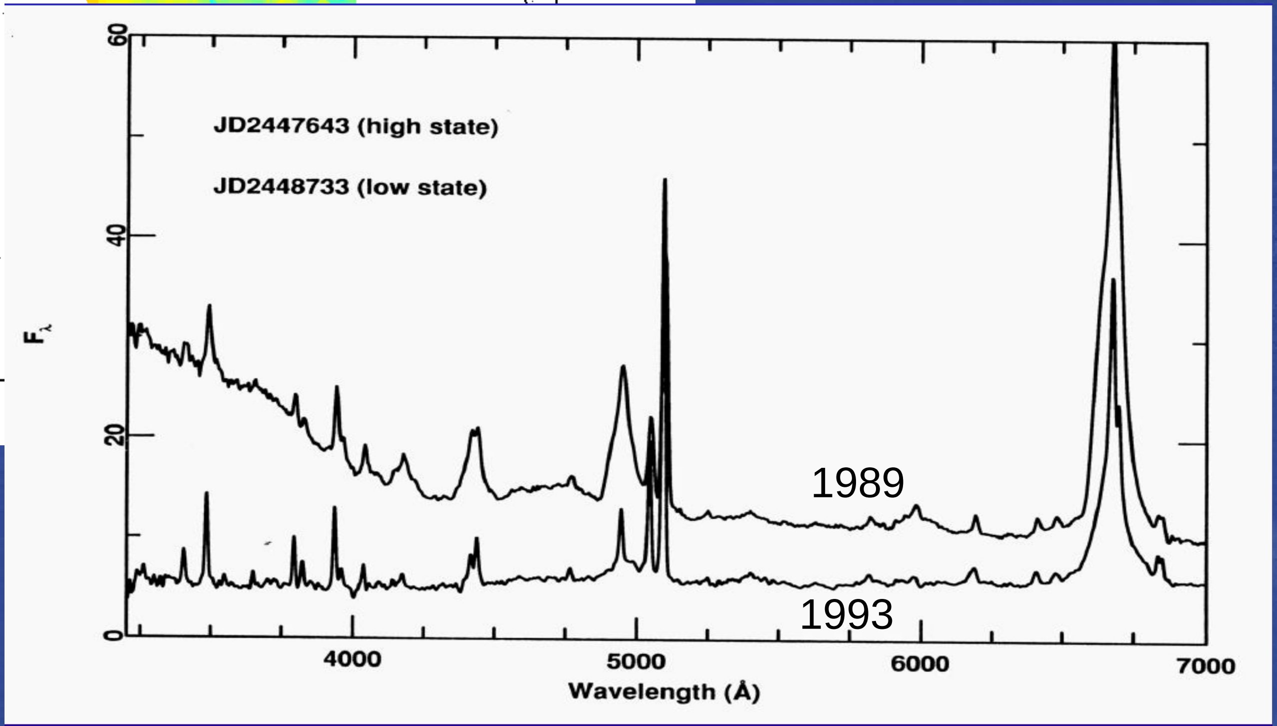

Variability of AGN emission lines

HET variability campaign of MRK 110 (Kollatschny et al. 2001)

long-term continuum light curve

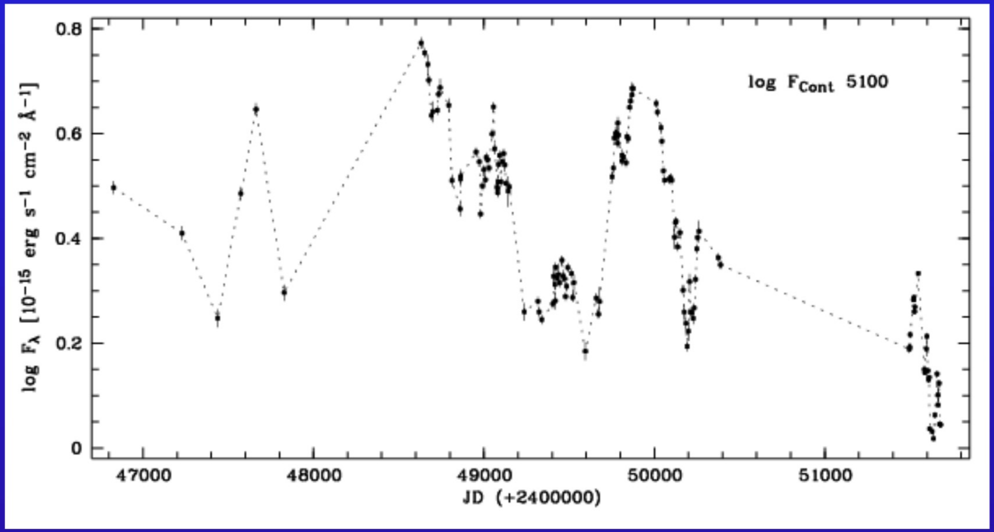

1987

2000

Mrk110 spectra taken between 1999 Nov. and 2000 May

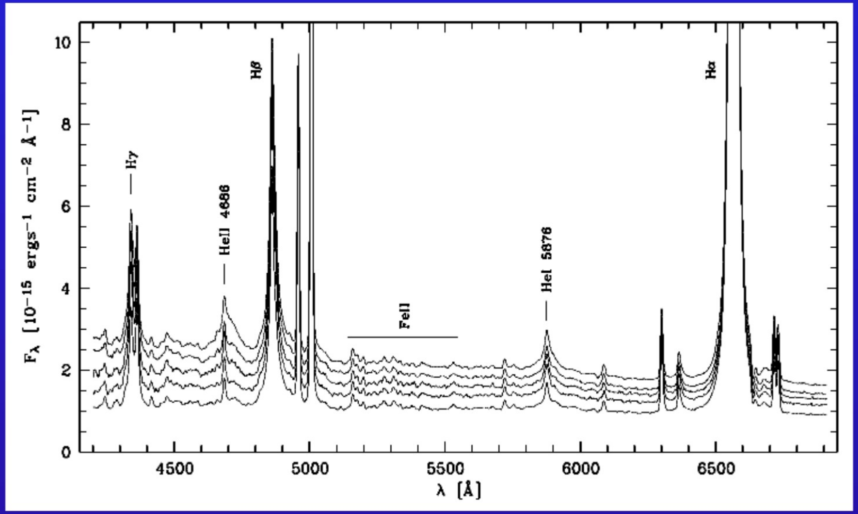

9.2m Hobby-Eberly Telescope at McDonald Observatory
S/N >100

Variability of AGN emission lines

HET variability campaign of Mrk 110 (Kollatschny et al. 2001)

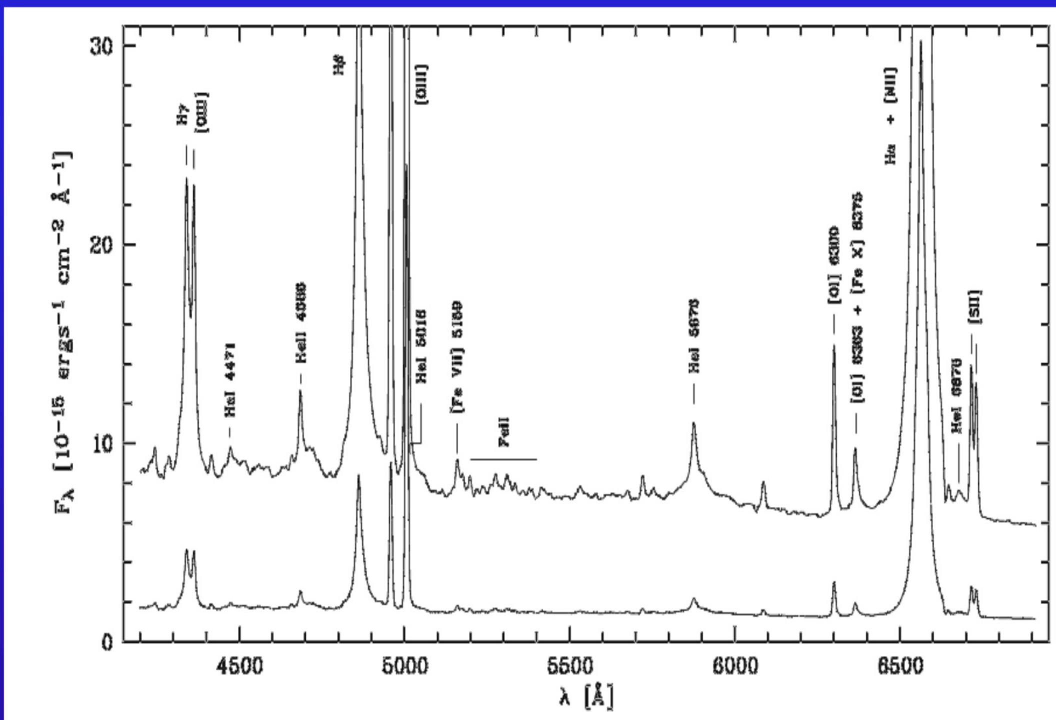

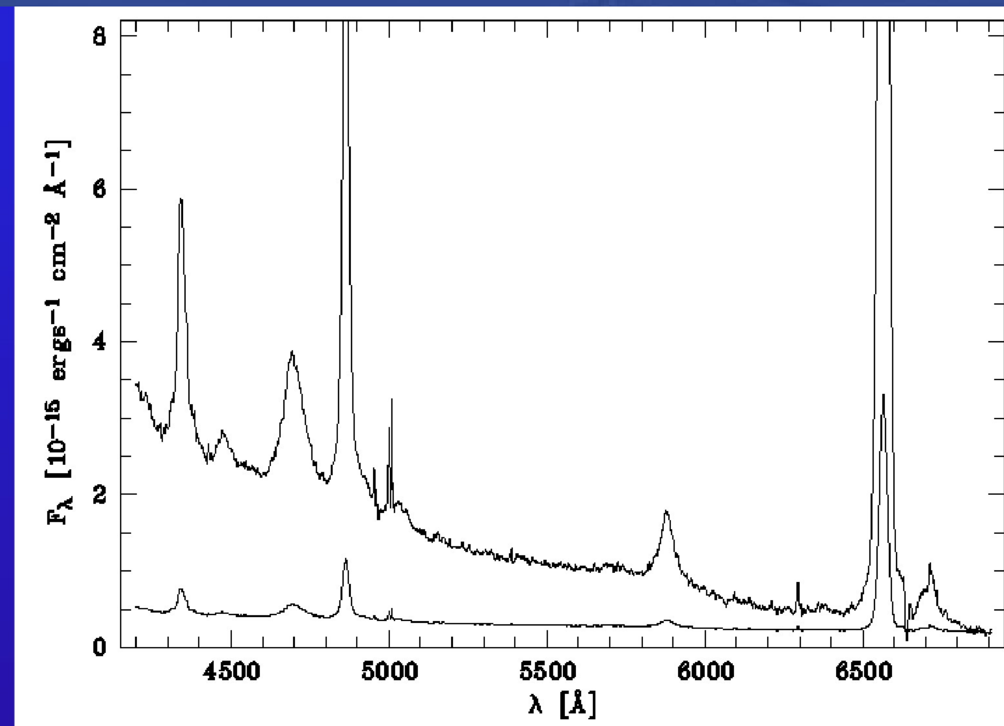

Mean spectrum of Mrk110 for 24 epochs from Nov. 1999 through May 2000

Rms spectrum

- the rms spectrum shows the variable part of the spectrum

Variability of AGN emission lines

HET variability campaign of MRK 110 (Kollatschny et al. 2003)

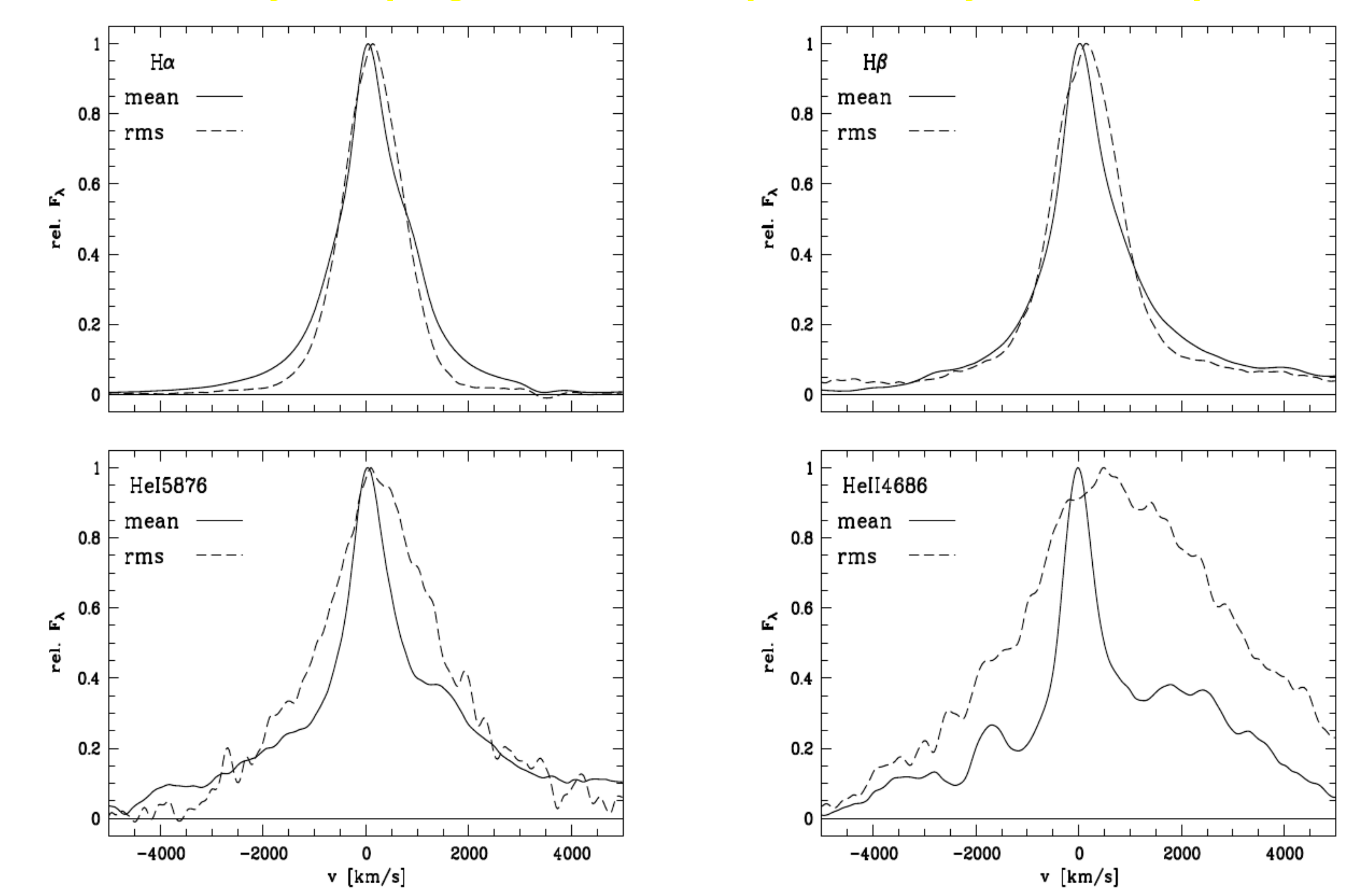

Normalized mean (dashed lines) and rms (solid lines) Balmer and Helium emission line profiles.

Black hole mass estimation

- Inclination dependent:

$$M_{\rm orbital} = f v^2 G^{-1} R.$$

$$M_{\rm orbital} = 1.8 \pm 0.4 \times 10^7 M_\odot.$$

Table 1. Rms line widths (FWHM) of our strongest emission lines: Hα, Hβ, HeIλ5876, and HeIIλ4686; differential redshift of rms line centers $\Delta\, v_{\rm cent}$(rms) ; cross-correlation lags τ and central black hole mass estimation $M_{\rm grav}$ derived from gravitational redshift.

Line (1)	FWHM(rms) [km s^{-1}] (2)	$\Delta\, v_{\rm cent}$(rms) [km s^{-1}] (3)	τ [days] (4)	$M_{\rm grav}$ [$10^7 M_\odot$] (5)
HeII	4444 $\pm$ 200	541 $\pm$ 60	3.9 $\pm$ 2	13 $\pm$ 3
HeI	2404 $\pm$ 100	186 $\pm$ 60	10.7 $\pm$ 6	12 $\pm$ 4
Hβ	1515 $\pm$ 100	118 $\pm$ 50	24.2 $\pm$ 4	17 $\pm$ 4
Hα	1315 $\pm$ 100	74 $\pm$ 50	32.3 $\pm$ 5	14 $\pm$ 5

- Inclination independent – from the redshift (Zheng & Sulentic 1990, ApJ 350, 512):

$$M_{\rm grav} = c^2 G^{-1} R \Delta z.$$

$$M_{\rm grav} = 14 \pm 3 \times 10^7 M_\odot.$$

$$\Rightarrow \quad M_{\rm orbital} / M_{\rm grav} = \sin^2 i$$

Variability of AGN emission lines

HET variability campaign of MRK 110 (Kollatschny et al. 2003)

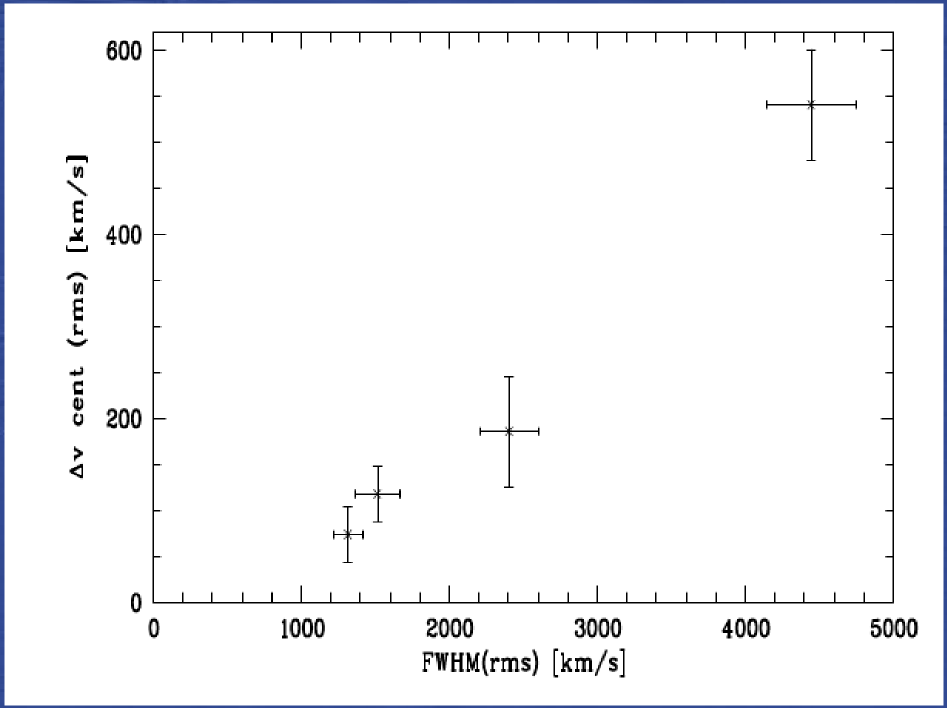

Relative redshift of Hα, Hβ, HeIλ5876, and HeIIλ4686 rms line centers as a function of rms line width (FWHM).

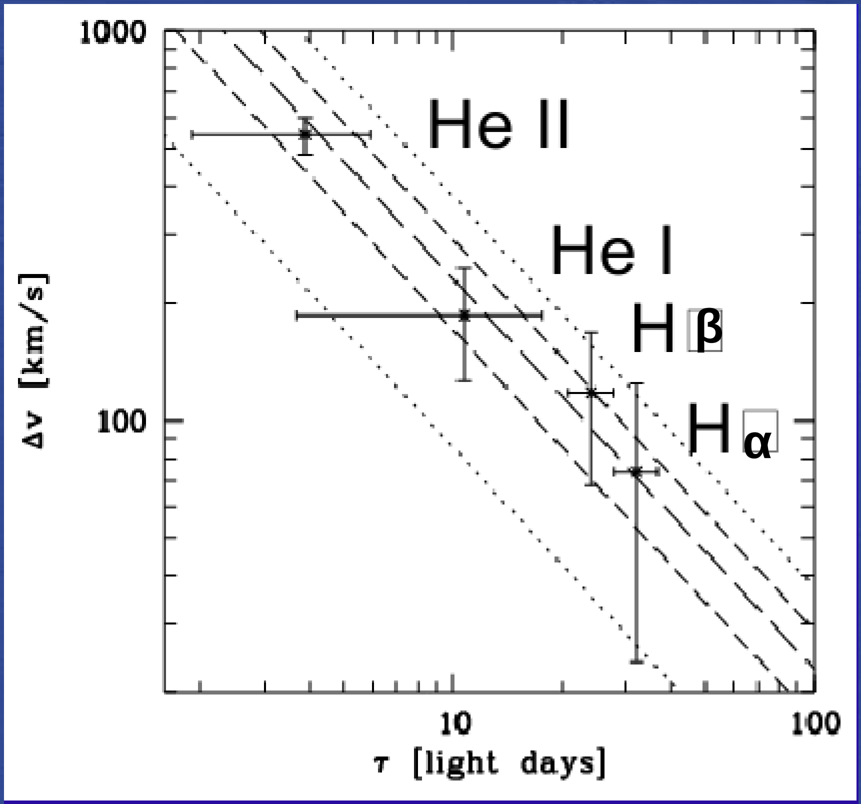

Line shift vs. distance
Dotted and dashed curves: computed lines of gravitational redshift for masses of 5. - 22. $x10^7 M_\odot$ (from bottom to top).

Variability of AGN emission lines

WHT and INT variability campaign of NGC 4593 (Kollatschny et al. 1997, A & A, 323,5)

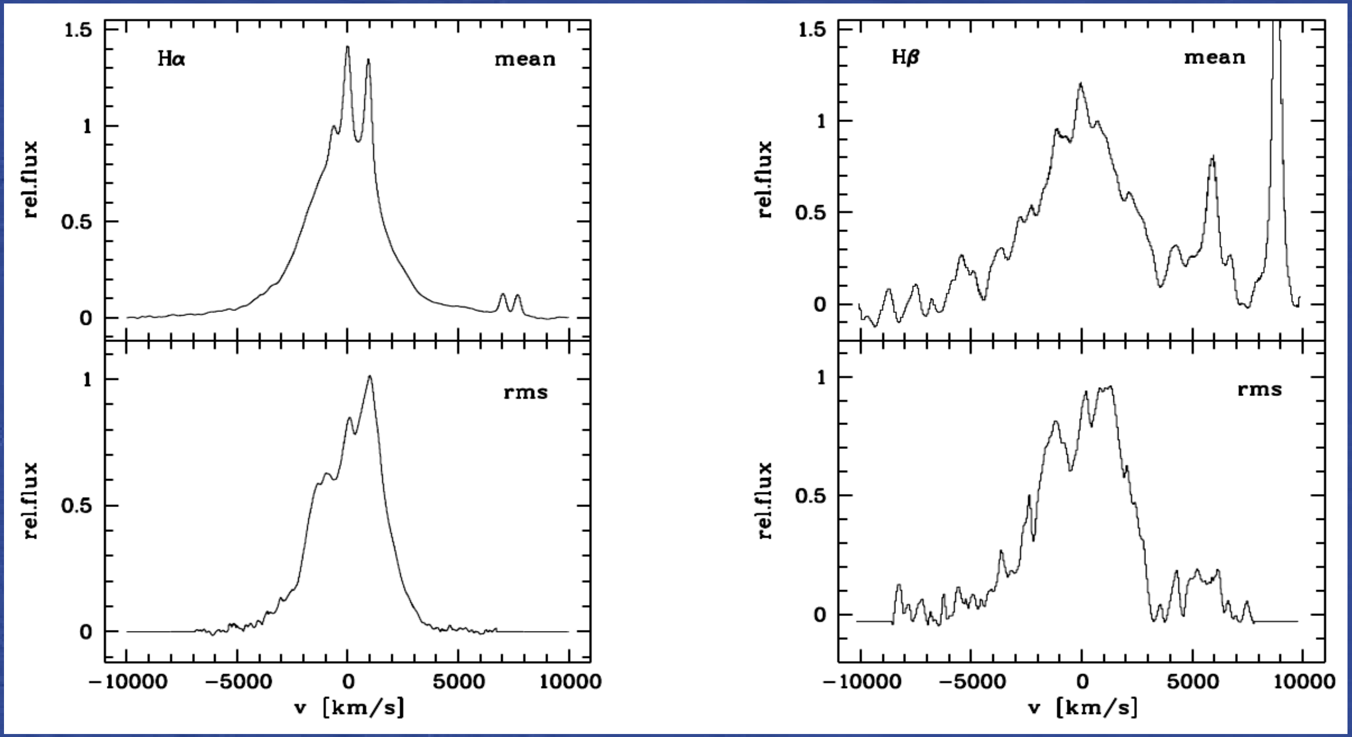

M_{grav}:

$$M \leq c^2 G^{-1} R \Delta z$$

$$M \leq 2.3\ 10^7 M_\odot$$

M_{orbit}:

$$M = \frac{3}{2} v^2 G^{-1} R$$

$$M = 1.4\ 10^7 M_\odot$$

Black hole mass vs. galactic (systematic) redshift

Pop A+Pop B

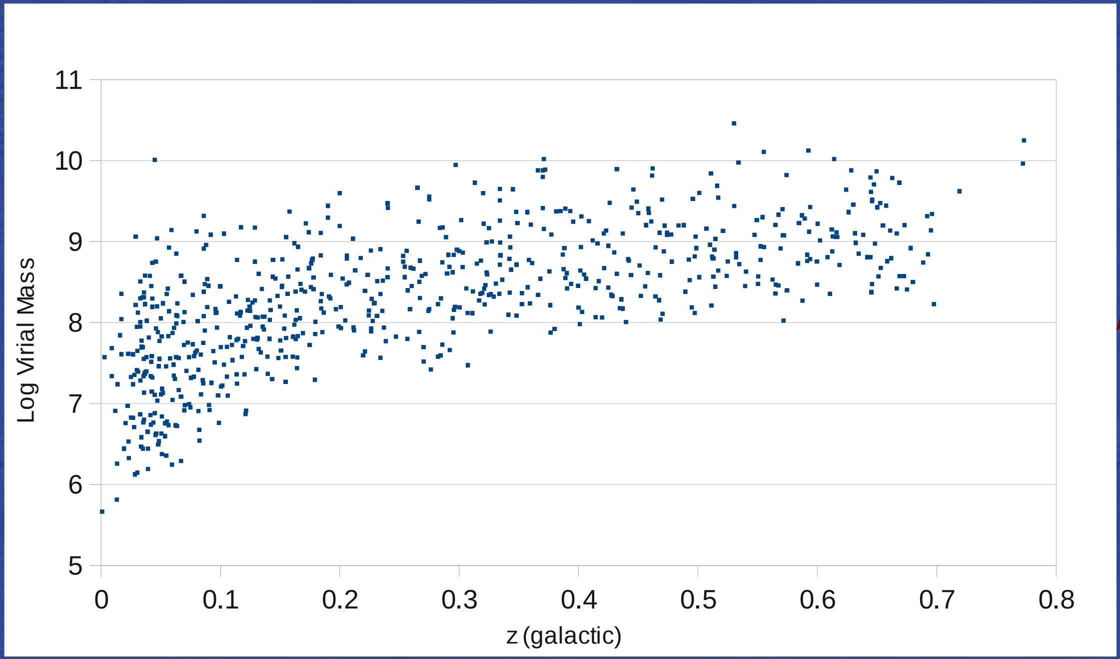

Virial Mass(Sulentic & Marziani)

Mass from gravitational redshift

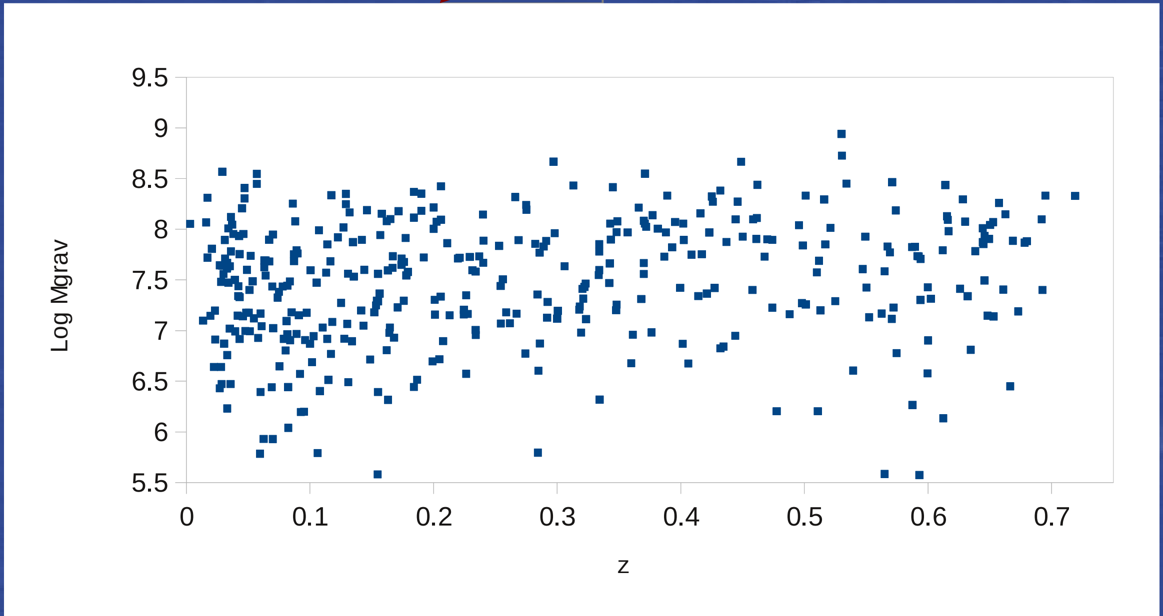

$$M_{grav}=c^2G^{-1}R\Delta z$$

Orientation of the accretion disk

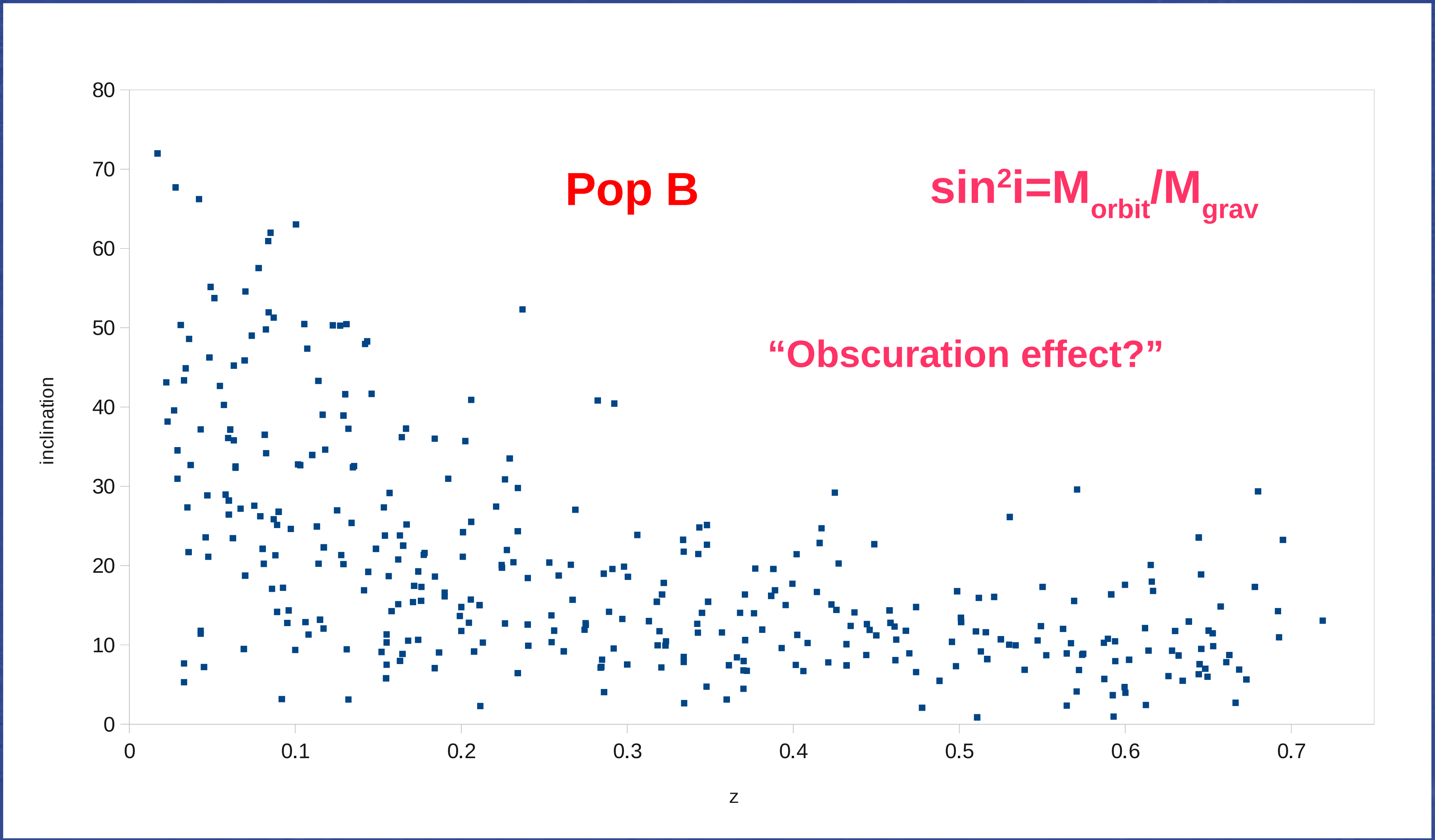

Summary

Variable emission line component that originate close to a black hole might show the redshift that can be explained as a gravitational redshift.

Gravitational redshift can be used to estimate the mass of a super-massive black hole in the center of a galaxy, that represent an estimation independent on the geometry and an inclination of the accretion disk, in a difference to the orbital mass obtained from the width of the emission line.

The ratio between the masses obtained using gravitation redshift and FWHM of the line, can give the orientation angle i of the accretion disk and therefore the spin orientation of the galaxy.